Available online at www.sciencedirect.com
SCIENCE DIRECT®
PERGAMON
International Journal of Heat and Mass Transfer 46 (2003) 4885–4898
International Journal of HEAT and MASS TRANSFER
www.elsevier.com/locate/ijhmt

Fluid dynamical view of pressure checkerboarding problem and smoothing pressure correction on meshes with colocated variables

A.W. Date *

Mechanical Engineering Department, Indian Institute of Technology, Bombay, Mumbai 400076, India

Received 16 December 2002; received in revised form 25 April 2003

Abstract

This paper presents derivation of the pressure correction equation appropriate for colocated grids within the framework of the SIMPLE algorithm. It is shown that checkerboard prediction of pressure can be prevented by employing algebraic *smoothing* pressure correction [Numer. Heat Transfer, Part B 29 (1996) 441] that is very simple to implement on both the structured as well as unstructured grids. The ability of the smoothing correction (which is shown to be independent of transformations of the system of coordinates) in providing the necessary dissipation is explained and the connection of the former with requirements of the Stokes's laws is established.

Keywords: SIMPLE algorithm; Smoothing pressure correction; Structured and unstructured meshes; Colocated variables; Navier–Stokes equations

1. Introduction

1.1. The problem considered

In the solution of Navier–Stokes equations in their discretised form, the discretised velocities that are used to satisfy mass conservation equation (from which the pressure distribution is determined) should also satisfy the momentum equations. When this requirement is implemented explicitly, there results the well known *staggered grid* arrangement for location of pressure and velocity variables. The SIMPLE [3] and the MAC [4] methods employed this strategy on structured grids. Later, Baliga and Patankar [1,2] employed this strategy on unstructured grids.

In the computation of 3-dimensional flows in complex geometries using *structured* curvilinear or *unstructured* grids, several practical advantages are achieved by emloying *non-staggered* or *colocated* grids in which the velocities and the pressure (as well as other scalars) are stored/defined at the same grid location (that is, at the nodes). Though practically attractive, the colocated arrangement is beset with one major difficulty. Thus, when

(a) the mass conserving control-volume (or cell-face) velocities are (one- or multi-dimensionally) linearly interploated between neighbouring momentum conserving nodal velocities and,
(b) the pressure gradient appearing in the momentum equations written for the nodal velocities is represented by straight-forward central-differencing (the so called 2-$\Delta\xi$ differencing) approximation,

the predicted pressure distribution shows checkerboard or zig-zag [6] variation whereas the predicted velocities are often smooth. The nature of this zig-zag variation is shown in [7] for structured Cartesian grids and in [8] for unstructured grids. Further, Date [7] has shown that the extent of zig-zagness reduces as the mesh size is refined and that if the true pressure variation were to be spatially linear or constant, no zig-zagness occurs in the predicted pressure. These findings contrast the

* Tel.: +91-22-572-2545; fax: +91-22-572-3480.
E-mail address: awdate@me.iitb.ac.in (A.W. Date).

0017-9310/$ - see front matter
doi:10.1016/S0017-9310(03)00332-6

Nomenclature

AE, AW, AN, AS, AP, BP	coefficients in discretised equations
D_x, D_y	coefficients in pressure correction equation
$\dot{m}$	mass source
p	pressure
R	residual
S	source term
u	x-direction velocity
v	y-direction velocity
w	z-direction velocity

Greek symbols

α	under-relaxation factor for velocity
β	under-relaxation factor for pressure
μ	dynamic viscosity
Δ	control volume
Δx, Δy	control volume dimensions
ρ	density
Φ	general variable
λ	second viscosity coefficient
λ_1	multiplier of p–$\bar{p}$
σ	normal stress
τ	shear stress

Suffixes

P, N, S, E, W	refers to grid nodes
n, s, e, w	refers to cell-faces
f	refers to cell-face
m	refers to mass conservation
s	refers to smoothing
x, y, z	refers to x-, y- and z-directions

Superscripts

l	iteration counter
o	old time
u, v	refers to u, v momentum equations
—	multidimensional average
$'$	correction

notional illustration of checkerboarding or zig-zagness described in [6,19].

There have been three cures for the prevention of the problem of pressure zig-zagness suggested so far depending on the identified cause. The first and, the most popular one, was suggested by Rhie and Chow [13] who traced the cause of the problem to imperfect representation of the cell-face velocities that satisfy the mass conservation. In this sense, the cure is sought in response to the situation (a) described above. They therefore suggested a modelling expression for the cell-face velocities involving one-dimensional interpolated pressure gradients. The notion embodied in the *equal-order* pressure gradient evaluation suggested by Prakash and Patankar [5] is similar. Majority of the publications in the last two decades (see, for example, [5,13–17]) have adhered to this form of cure on both structured as well as unstructured grids. The second cure viewed the problem of zig-zagness as one that is caused by the so called velocity–pressure de-coupling. This implies that when the pressure gradient appearing in the nodal momentum equations is represented as in (b) above, the pressure p_P (say) at the node P does not appear in the discretised equations for u_P and v_P. Date [7] therefore proposed a higher-order discretisation for the pressure gradient so that the discretised equations are infact sensitised to p_P.

Both the above cures lack *fluid dynamical* justification for the cure as well as for the cause of the problem of zig-zagness. Date [9,10] therefore re-derived the pressure-correction equation appropriate for colocated grids which led to identification of a *smoothing* pressure correction. While the effectiveness of this third cure was rigorously demonstrated along with the demonstartion of its simplicity, the fluid dynamical basis of the cure has remained unexplained. The main purpose of this paper is therefore to explain, in somewhat detailed and longish pedagogical tone, the cure prescribed by Date [9,10].

The pedagogical tone is prompted first by the fact that several CFD researchers have sought clarification about the author's cure. Second and, more importantly, it turns out that several variants of Rhie and Chow [13] cure produce smooth pressure distributions on coarse grids and the problem itself disappears when the mesh size is refined. The same applies to the second cure of Date [7]. This compounds the problem of understanding of the main issues even further. Third, neither of the three cures bring any appreciable economic advantage when accurate solutions employing fine mesh sizes are of interest. All cures merely mimic the *satisfaction* of predicting smooth pressure distributions on *coarse* colocated grids that the staggered grid approach so naturally provides.

1.2. The present contribution

In this paper, Date's [9,10] cure is explained from a fluid-dynamical stand point. Several derivations (not found in [9,10]) applicable to structured and unstructured grids are therefore presented along with the discussion of the issues (often overlooked by researchers) pertaining to node-centered and cell-face-centered dispositions of structured grids. It is shown that the so called *fourth-order dissipation* is also a natural outcome of the fluid dynamical view. A brief version of the present paper is published in [11].

The overall discussion is first carried out with reference to structured Cartesian grids within the framework of the SIMPLE algorithm. So the familiarity with the latter is assumed. For complete understanding of the derivations, the reader will need to carry out some algebra him/herself.

2. Navier–Stokes equations

2.1. Equations of motion

As presented in Schlichting [25], the equations of motion in non-conservative form can be written as

$$\frac{\mathrm{D}\rho}{\mathrm{D}t} = -\rho\nabla\cdot V = -\rho\left(\frac{\partial u}{\partial x}+\frac{\partial v}{\partial y}+\frac{\partial w}{\partial z}\right) \tag{1}$$

$$\rho\frac{\mathrm{D}u}{\mathrm{D}t} = \frac{\partial\sigma_x}{\partial x}+\frac{\partial\tau_{yx}}{\partial y}+\frac{\partial\tau_{zx}}{\partial z} \tag{2}$$

$$\rho\frac{\mathrm{D}v}{\mathrm{D}t} = \frac{\partial\tau_{xy}}{\partial x}+\frac{\partial\sigma_y}{\partial y}+\frac{\partial\tau_{zy}}{\partial z} \tag{3}$$

$$\rho\frac{\mathrm{D}w}{\mathrm{D}t} = \frac{\partial\tau_{xz}}{\partial x}+\frac{\partial\tau_{yz}}{\partial y}+\frac{\partial\sigma_z}{\partial z} \tag{4}$$

where, using Tensor notation, the shear stresses are specified by

$$\tau_{ij} = \mu\left(\frac{\partial u_i}{\partial x_j}+\frac{\partial u_j}{\partial x_i}\right) \tag{5}$$

and the normal stresses are given by

$$\sigma_x = -p+\sigma'_x = -p+q+2\mu\frac{\partial u}{\partial x} \tag{6}$$

$$\sigma_y = -p+\sigma'_y = -p+q+2\mu\frac{\partial v}{\partial y} \tag{7}$$

$$\sigma_z = -p+\sigma'_z = -p+q+2\mu\frac{\partial w}{\partial z} \tag{8}$$

In the above normal stress expressions, σ' is called the deviotoric stress and the quantity q in its definition is newly introduced in this paper. The significance of this quantity will become shortly clear. Schlichting [25] and Warsi [26], for example, define a space averaged pressure $\bar{p}$ as

$$\bar{p} = -\frac{1}{3}(\sigma_x+\sigma_y+\sigma_z) \tag{9}$$

Now, an often overlooked *requirement* of the Stokes's relations is that, in a continuum, $\bar{p}$ must equal the point value of pressure p and the latter, in turn, must equal the thermodynamic pressure pth. Thus,

$$\bar{p} = p = p\mathrm{th} = p-q-\frac{2}{3}\mu\nabla\cdot V \tag{10}$$

We now consider different flow cases to derive significance of q.

1. *Case 1*. ($V=0$) In this *hydrostatic case*

$$\bar{p} = p-q \tag{11}$$

But in this case, p can only vary linearly with x, y, z and therefore the point value of p exactly equals its space averaged value $\bar{p}$ in both continuum as well as discretised space and hence $q=0$ exactly.

2. *Case 2*. ($\mu=0$ or $\nabla\cdot V=0$) Clearly when $\mu=0$ (inviscid flow) or $\nabla\cdot V=0$ (constant density incompressible flow) equation (11) holds. But, in this case, since fluid motion is considered, p can vary arbitrarily with x, y and z and therefore p may not equal $\bar{p}$ in a discrete space. However, without violating the continuum requirement, we may set

$$q = \lambda_1(p-\bar{p}) \tag{12}$$

where λ_1 is an arbitrary constant. In most textbooks, where continuum is assumed, λ_1 is trivially set to zero.

3. *Case 3*. ($\mu\neq 0$ and $\nabla\cdot V\neq 0$) This case represents either compressible flow where density is a function of both temperature and pressure or incompressible flow with temperature dependent density. Thus,

$$\bar{p} = p-\left(q+\frac{2}{3}\mu\nabla\cdot V\right) \tag{13}$$

In this case, Stokes's requirement is satisfied if we set

$$q = \lambda_1(p-\bar{p})+\lambda\nabla\cdot V \tag{14}$$

where λ is the well-known second viscosity coefficient whose value is set to $-(2/3)\mu$ even in a continuum.

It is instructive to note the reason for setting $\lambda=-(2/3)\mu$. For, if this was not done, it would amount to

$$(1-\lambda_1)(p-\bar{p})\nabla\cdot V = \left(\lambda+\frac{2}{3}\mu\right)(\nabla\cdot V)^2 \tag{15}$$

Clearly, therefore, the system will experience *dissipation* (or reversible work done at finite rate since $\nabla\cdot V$ is associated with the rate of volume change, see equation (1).) even in an isothermal flow [25,26]. This is, of course, highly improbable. [1] It is now easy to understand that the same interpretation can be afforded to $\lambda_1(p-\bar{p})$ part of q in Eq. (12) or (14).

[1] Schlichting [25] shows this improbability by considering the case of an isolated sphere of a compressible isothermal gas subjected to uniform normal stress. Now if λ is not set to $-(2/3)\mu$, the gas will undergo oscillations.

Before taking up the issue of zig-zag pressure prediction via *discretised* Navier–Stokes equations, following observations are made.

1. Whenever q is finite (non-zero), the system will experience dissipation and the requirement $p = \bar{p} = p$th will not hold. As shown above, the hydrostatic case is the only one in which q is identically zero in both the discretised space as well as continuum. In all other cases when spatial variations of p may in general depart from linearity, q must be specially tailored both in a continuum as well as in a discrete space.
2. In an isotropic fluid, q (as it appears in each of the normal stress expressions) cannot have directional properties. In other words, q must be invariant under transformation of the system of coordinates. In all cases considered above, this requirement is also satisfied. This observation, it will be shown, has bearing on the Rhie and Chow [13] interpolation scheme.

2.2. Discretised Navier–Stokes equations

In all further discussion, we consider 2-dimensional flows and write the N–S equations in conservative form as

$$\frac{\partial \rho}{\partial t} + \frac{\partial(\rho u_{\mathrm{f}})}{\partial x} + \frac{\partial(\rho v_{\mathrm{f}})}{\partial y} = 0 \tag{16}$$

$$\frac{\partial \rho u}{\partial t} + \frac{\partial(\rho u_{\mathrm{f}} u)}{\partial x} + \frac{\partial(\rho v_{\mathrm{f}} u)}{\partial y} = -\frac{\partial p}{\partial x} + \frac{\partial}{\partial x}\left(\mu \frac{\partial u}{\partial x}\right) + \frac{\partial}{\partial y}\left(\mu \frac{\partial u}{\partial y}\right) \tag{17}$$

$$\frac{\partial \rho v}{\partial t} + \frac{\partial(\rho u_{\mathrm{f}} v)}{\partial x} + \frac{\partial(\rho v_{\mathrm{f}} v)}{\partial y} = -\frac{\partial p}{\partial y} + \frac{\partial}{\partial x}\left(\mu \frac{\partial v}{\partial x}\right) + \frac{\partial}{\partial y}\left(\mu \frac{\partial v}{\partial y}\right) \tag{18}$$

The above equations [2] are discretised using control volume approach in which the equations are integrated over a finite chosen control volume. In Fig. 1, the chosen grid disposition with control volume surrounding node P (say) is shown. In this figure, the locations of the dotted lines (or the cell-faces) that define the control volumes are so chosen that they lie *midway* between the adjacent nodes. In this case, the nodes will not be at the geometric centre of the control volumes when non-uniform grids are chosen. [3]

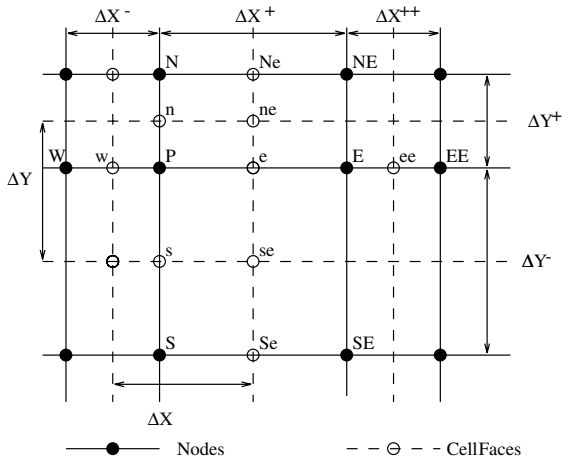

Fig. 1. Typical Cartesian structured grid—cell-faces are midway between the nodes.

Now assuming that all variables vary linearly between immediate grid nodes and that the source terms are uniform over the control volume, it can be shown that the discretised momentum equations will read as [6]

$$u_P = \frac{AE u_E + AW u_W + AN u_N + AS u_S - \Delta \partial p/\partial x + BP u_P^{\circ}}{AP^u + BP} \tag{19}$$

$$v_P = \frac{AE v_E + AW v_W + AN v_N + AS v_S - \Delta \partial p/\partial y + BP v_P^{\circ}}{AP^v + BP} \tag{20}$$

where the coefficients are defined as

$$AE = \left[\frac{\mu_{\mathrm{e}} \Delta y}{\Delta x^{+}} - \frac{\rho_{\mathrm{e}} u_{\mathrm{fe}}}{2}\Delta y\right]$$

$$AW = \left[\frac{\mu_{\mathrm{w}} \Delta y}{\Delta x^{-}} + \frac{\rho_{\mathrm{w}} u_{\mathrm{fw}}}{2}\Delta y\right] \tag{21}$$

$$AN = \left[\frac{\mu_{\mathrm{n}} \Delta x}{\Delta y^{+}} - \frac{\rho_{\mathrm{n}} v_{\mathrm{fn}}}{2}\Delta x\right]$$

$$AS = \left[\frac{\mu_{\mathrm{s}} \Delta x}{\Delta y^{-}} + \frac{\rho_{\mathrm{s}} v_{\mathrm{fs}}}{2}\Delta x\right] \tag{22}$$

$$AP^u = AP^v = AE + AW + AN + AS \tag{23}$$

$$BP = \frac{\rho_P^{\circ} \Delta}{\Delta t} \tag{24}$$

In deriving Eq. (23), the satisfaction of mass conservation over the control volume surrounding node P is implicit. From the above equations, it is clear that suffix 'f' is attached to velocities that appear at the *cell-faces*; velocities without suffix 'f' appear at the nodes. Further, coefficients A_i, $i = E, W, N, S$ are written in their raw (CDS) form; they can be altered for different convection schemes such as UDS, Power etc. [6].

[2] The significance of suffix 'f' will become shortly clear.

[3] Some researchers prefer to have nodes at the geometric centres of the control volumes. Then the cell-faces will not be midway between adjacent nodes. It will be shown later that this difference is, however, inconsequential to the main issues discussed in this paper.

All quantities appearing at the cell-faces (e, w, n and s) are now linearly interpolated in terms of their values at the nodal locations since when computing on colocated grids, all variables are stored at the nodal locations. For fluid properties μ and ρ, one dimensional linear interpolation suffices. For velocities, however, it will be shown later that multidimensional averaging may be preferred.

Now, the pressure gradient terms are evaluated by central-difference so that

$$\left.\frac{\partial p}{\partial x}\right|_P = \frac{p_e - p_w}{\Delta x} = \frac{p_E - p_W}{2\Delta x} \tag{25}$$

$$\left.\frac{\partial p}{\partial y}\right|_P = \frac{p_n - p_s}{\Delta x} = \frac{p_N - p_S}{2\Delta y} \tag{26}$$

When the above equations are substituted in Eqs. (19) and (20), it becomes clear that u_P and v_P are not sensitised to p_P. This is known as the velocity–pressure decoupling problem that eventually leads to the zig-zag pressure prediction.

3. Pressure smoothing on Cartesian grids

3.1. Mass conserving pressure correction equation

In the SIMPLE algorithm [3], while the velocities are determined from Eqs. (19) and (20) with a guessed pressure field, the latter is sought to be iteratively corrected via satisfaction of the mass conservation equation (16) over the control volume surrounding node P. This is done by deriving the mass conserving pressure correction equation. This equation must be identical for both the staggered grid as well as the colocated grid arrangements because the pressure is stored at the same grid node location in either arrangements. Here, the derivation of this equation as carried out by Date [9] is repeated for completeness including the case of unsteady flows.

In unsteady flows, at a new time step, nodal velocities u_P and v_P are calculated from Eqs. (19) and (20). Their counterparts at cell-face locations e and w (where u_f is defined) and n and s (where v_f is defined) will read as

$$u_f^{l+1} = \frac{\sum A_i u_{fi}^{l+1} - \Delta \partial p^{l+1}/\partial x}{AP^{u_f} + BP} + \frac{BP}{AP^{u_f} + BP} u_f^{o} \tag{27}$$

$$v_f^{l+1} = \frac{\sum A_i v_{fi}^{l+1} - \Delta \partial p^{l+1}/\partial y}{AP^{v_f} + BP} + \frac{BP}{AP^{v_f} + BP} v_f^{o} \tag{28}$$

where l is iteration level and $\sum A_i u_i$ and $\sum A_i v_i$ simply represent summation over immediate neighbours of locations of u and v for which equations (27) and (28) are written. Thus, when equation (27), for example, is written for cell-face e, i = ee, w, Ne and Se.

When steady flow is considered, the above equations still apply if we set $BP = 0$ (or, $\Delta t = \infty$). However, in an iterative procedure, under-relaxation is often necessitated. This need can be met in two ways. In the first, one may regard the steady flow as falsely unsteady and specify a false time step Δt so that $BP > 0$. In the second method, the usual *global* under-relaxation factors (say, α) are used. Then it is possible to show that in the first alternative, $\alpha = AP/(AP + BP)$. But here, α will vary from node to node because AP and BP vary with node position. It is also possible to show that this variation in α is in the desirable direction; large when AP is small and small when AP is large. Whether variable or global under-relaxation is used is a matter of choice and does not in any way alter the discussion to follow.

Note that on colocated grids, Eqs. (27) and (28) are not actually solved but *imagined* to be solved. Now, the $l+1$ level velocities, it is expected, will satisfy the mass conservation equation. Thus

$$\frac{\partial \rho^{l+1}}{\partial t} + \frac{\partial (\rho u_f^{l+1})}{\partial x} + \frac{\partial (\rho v_f^{l+1})}{\partial y} = 0 \tag{29}$$

Substitution of Eqs. (27) and (28) in Eq. (29) therefore yields

$$\frac{\partial \rho^{l+1}}{\partial t} + \frac{\partial}{\partial x}\left[\frac{\rho^{l+1}\left\{\sum A_i u_{fi}^{l+1} - \Delta \partial p^{l+1}/\partial x + BP u_f^{o}\right\}}{AP^{u_f} + BP}\right] + \frac{\partial}{\partial y}\left[\frac{\rho^{l+1}\left\{\sum A_i v_{fi}^{l+1} - \Delta \partial p^{l+1}/\partial y + BP v_f^{o}\right\}}{AP^{v_f} + BP}\right] = 0 \tag{30}$$

In order to develop the pressure correction equation, we now write

$$u_f^{l+1} = u_f^{l} + u_f' \quad v_f^{l+1} = v_f^{l} + v_f' \quad p^{l+1} = p^{l} + p_m' \tag{31}$$

where p_m' is the *mass conserving* pressure correction. Substituting Eq. (31) in Eq. (30) yields [4]

$$\frac{\partial}{\partial x}\left[D_x \frac{\partial p_m'}{\partial x}\right] + \frac{\partial}{\partial y}\left[D_y \frac{\partial p_m'}{\partial y}\right] = \frac{\partial (\rho u_f^{l})}{\partial x} + \frac{\partial (\rho v_f^{l})}{\partial y} + \frac{\partial \rho^{l+1}}{\partial t} - \frac{\partial}{\partial x}[D_x R_{u_f}] - \frac{\partial}{\partial y}[D_y R_{v_f}] \tag{32}$$

where

$$D_x = \frac{\rho^{l+1}\Delta}{AP^{u_f} + BP} \quad D_y = \frac{\rho^{l+1}\Delta}{AP^{v_f} + BP} \tag{33}$$

and R_{u_f} and R_{v_f} are residuals per unit volume given by

$$R_{u_f} = \frac{(AP^{u_f} + BP)u_f^{l} - \sum A_i u_f^{l} i - BP u_f^{o}}{\Delta} + \frac{\partial p^{l}}{\partial x} \tag{34}$$

[4] In deriving this equation, the approximation $\sum A_i u_{fi}' = \sum A_i v_{fi}' = 0$ used in the SIMPLE algorithm has been invoked.

$$R_{v_f} = \frac{(AP^{v_f} + BP)v_f^l - \sum A_i v_f^l i - BPv_f^o}{\Delta} + \frac{\partial p^l}{\partial y} \tag{35}$$

The partial differential equation (32) is applicable to both staggered and colocated grids as well as to structured and unstructured meshes.

3.2. The staggered grid form

When Eq. (32) is discretised, u_f and R_{u_f} must be evaluated at the cell-faces e and w and likewise v_f and R_{v_f} must be evaluated at the cell-faces n and s. The discretised form is

$$APp'_{m,P} = AEp'_{m,E} + AWp'_{m,W} + ANp'_{m,N} + ASp'_{m,S} - \dot{m}_P + \dot{m}_R \tag{36}$$

where

$$AE = \frac{\rho_e^{l+1}\Delta^2 y}{(AP^{u_f} + BP)_e} \quad AN = \frac{\rho_n^{l+1}\Delta^2 x}{(AP^{v_f} + BP)_n} \text{ etc.} \tag{37}$$

$$\dot{m}_P = (\rho_e^{l+1}u_{fe}^l - \rho_w^{l+1}u_{fw}^l)\Delta y + (\rho_n^{l+1}v_{fn}^l - \rho_s^{l+1}v_{fs}^l)\Delta x + (\rho_P^{l+1} - \rho_P^o)\frac{\Delta}{\Delta t} \tag{38}$$

$$\dot{m}_R = (AER_{u_{fe}}\Delta x^+ - AWR_{u_{fw}}\Delta x^-) + (ANR_{v_{fn}}\Delta y^+ - ASR_{v_{fs}}\Delta y^-) \tag{39}$$

Note, however, that when the momentum equations are fully converged, R_{u_f} and R_{v_f} are rendered zero since the overall procedure solves Eqs. (27) and (28) for the cell-face velocities u_f and v_f. It is for this reason that the $\dot{m}_R$ is set to zero *even* during the iterative procedure. Effectively, therefore, the applicable *differential* equation for staggered grids can be written as

$$\frac{\partial}{\partial x}\left[D_x\frac{\partial p'_m}{\partial x}\right] + \frac{\partial}{\partial y}\left[D_y\frac{\partial p'_m}{\partial y}\right] = \frac{\partial(\rho u_f^l)}{\partial x} + \frac{\partial(\rho v_f^l)}{\partial y} + \frac{\partial \rho^{l+1}}{\partial t} \tag{40}$$

It is instructive to note that the above equation was derived via an alternative route in the original paper by Patankar and Spalding [3]. Without elaboration, we note that Eq. (40) is solved subject to boundary condition

$$\left.\frac{\partial p'_m}{\partial n}\right|_{\text{boundary}} = 0 \tag{41}$$

where n is normal to the boundary.

3.3. The unsuccessful colocated grid form

Since the above staggered grid form enjoyed success at smooth pressure prediction even on coarse grids, it was readily adopted for the colocated grids as well with $\dot{m}_R = 0$. The only change made was that the cell-face velocities were replaced by their interpolated (averaged) counterparts. That is, u_{fe}, for example, was replaced by $\bar{u}_e = 0.5(u_P + u_E)$, etc. Thus, $\dot{m}_P$ was written as

$$\bar{\dot{m}}_P = (\rho_e^{l+1}\bar{u}_e^l - \rho_w^{l+1}\bar{u}_w^l)\Delta y + (\rho_n^{l+1}\bar{v}_n^l - \rho_s^{l+1}\bar{v}_s^l)\Delta x + (\rho_P^{l+1} - \rho_P^o)\frac{\Delta}{\Delta t} \tag{42}$$

and the effective pressure correction equation read as

$$\frac{\partial}{\partial x}\left[D_x\frac{\partial p'_m}{\partial x}\right] + \frac{\partial}{\partial y}\left[D_y\frac{\partial p'_m}{\partial y}\right] = \frac{\partial(\rho^{l+1}\bar{u}^l)}{\partial x} + \frac{\partial(\rho^{l+1}\bar{v}^l)}{\partial y} + \frac{\partial \rho^{l+1}}{\partial t} \tag{43}$$

When the above equation was solved with boundary condition (41), the predicted pressure distribution showed zig-zagness in a general flow. However, an important observation noted in [7] is that no zig-zagness is predicted if the true pressure distribution was linear or constant.

The reader can verify these experiences by considering simple flows. Thus, if fully developed steady laminar flow between parallel plates is computed as a two-dimensional elliptic flow in which parabolic velocity profile is prescribed at inlet and zero-gradient boundary condition is prescribed on velocity at exit, it will be found that Eq. (43) along with Eqs. (19) and (20) does indeed predict linear pressure distribution in the streamwise direction and constant pressure in the transverse direction while parabolic axial velocity profile is predicted at all axial locations as would be expected. Date [7] considered buoyancy affected steady elliptic flow in a right angled corner for which, with artificial boundary conditions, Shih and Ren [23] formulated an exact solution. In this flow, at high Rayleigh numbers, again the pressure distribution in the direction of gravity is linear and that in the horizontal direction is constant. Date [7] showed that Eq. (43) was indeed successful in reproducing the exact solution.

On the other hand, if one considered a steady one-dimensional flow in a pipe with mass injection at constant rate through the walls, then the exact solution shows that axial velocity must increase linearly with the streamwise coordinate whereas the pressure variation must be parabolic. Date [7] showed that if staggered grids were employed with Eq. (40), the predicted pressure distribution on coarse grid was indeed smooth (but not accurate due to grid coarseness) but, with colocated grids and equation (43), the predicted pressure distribution showed zig-zagness on coarse grids because the true pressure distribution departed from linearity.

The nature of zig-zagness is further demonstarted here by considering the well known steady flow in a square lid-driven cavity. In Fig. 2 computed vertical mid-plane values of $(p - p_{x=0.5,y=1})$ are plotted along the x-axis. The vertical coordinate is along the y-axis. Three

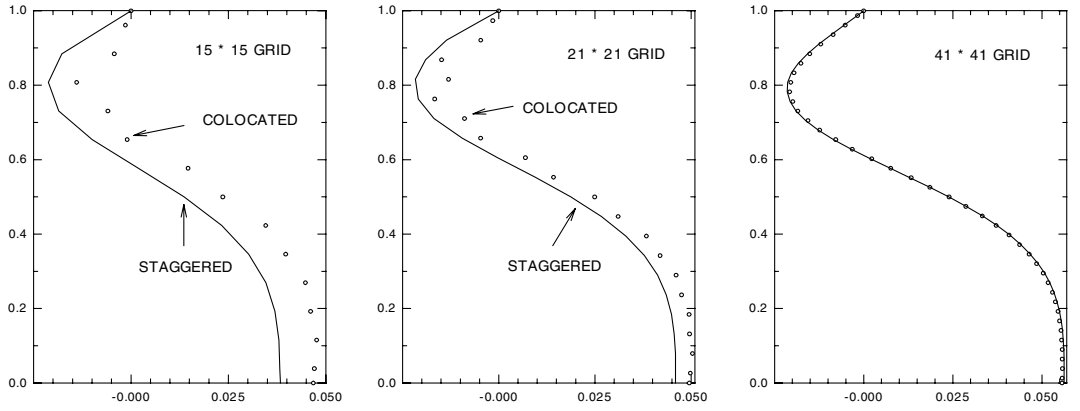

Fig. 2. Pressure variation at $X = 0.5$, $Re = 100$, square cavity with a moving lid.

grid sizes (15×15, 21×21 and 41×41) are used. The lines represent the staggered grid solutions and the colocated grid solutions are shown by open circles. It is seen that on coarser grids, predicted pressure distribution on colocated grids is zig-zag whereas the staggered grid pressure distributions are smooth. The zig-zagness is seen to be more pronounced in regions where the staggered grid pressure distribution departs considerably from linearity. At the finest mesh size, however, there is hardly any difference between the staggered and the colocated grids solutions, both being nearly equally smooth.

The above examples conclusively demonstrate that the problem of zig-zagness occurs only when coarse grids are used and when the true pressure departs from linearity. It will be shown in a later section that zig-zagness is a result of artificial dissipation introduced in the system. For removal of zig-zagness, therefore, this dissipation must be countered.

3.4. The popular successful colocated grid forms

Contrary to the above conclusion, the great majority of publications of the past two decades still view the problem of zig-zagness as being caused by imperfect cell-face velocity interpolation and accept the validity of Eq. (40) on colocated grids. Thus, with $\dot{m}_R = 0$, Eq. (38) is used in the evaluation of source term in Eq. (36) and u_{fe}, for example, was modelled by Rhie and Chow [13] as

$$u_{\mathrm{fe}} = \bar{u}_{\mathrm{e}} - \frac{D_x}{\rho}\left[\left.\frac{\partial p}{\partial x}\right|_{\mathrm{e}} - \left.\frac{\overline{\partial p}}{\partial x}\right|_{\mathrm{e}}\right] \tag{44}$$

where

$$\bar{u}_{\mathrm{e}} = \frac{1}{2}(u_P + u_E) \tag{45}$$

$$\left.\frac{\overline{\partial p}}{\partial x}\right|_{\mathrm{e}} = \frac{1}{2}\left[\left.\frac{\partial p}{\partial x}\right|_P + \left.\frac{\partial p}{\partial x}\right|_E\right] \tag{46}$$

There are numerous variants of the above form to warrent mention here. But, two alternative forms will be mentioned. The first, by Peric [19], replaced nodal velocities u_P and u_E by their discretised forms (see Eq. (19)) so that the resulting expression read as

$$u_{\mathrm{fe}} = \frac{1}{2}\left[\left.\frac{\sum A_i u_i}{AP^u + BP}\right|_P + \left.\frac{\sum A_i u_i}{AP^u + BP}\right|_E\right] - \frac{D_x}{\rho}\left.\frac{\partial p}{\partial x}\right|_{\mathrm{e}} \tag{47}$$

The second, by Thiart [22], evaluated u_{fe} from analytical solution to the one-dimensional conduction-convection problem introduced by Spalding [21]. Thus, the cell-face velocity was determined from a truncated momentum equation. When Eqs. (44), (47) or analytical solution is used, zig-zagness is indeed removed on a coarse grid but, some embarassments are encountered.

1. The predicted solutions for u, v and p show dependence on global under-relaxation factor α used in the momentum equations. This dependence was cured by Majumdar [20] while employing the Peric model expression (47). This matter will be further explained in a later subsection.
2. Miller and Schmidt [17] carried out computations of a backward-facing-step problem using staggered and colocated grids of identical dimensions employing Eq. (44) on the colocated grids. They found that u_{fe}, as predicted by Eq. (44), not only did not match with that predicted by the staggered grid procedure, u_{fe} did not even remain bounded between u_P and u_E. The analytical solution used by Thiart, on the other hand, will ensure this boundedness. Date [7] has explained this problem of unboundedness.
3. There is no theoretically rigorous proof for introduction of the pressure gradient terms in Eq. (44). It is essentially of a *it works* variety.
4. The analytical solution used by Thiart [22] leads to extremely complex evaluations of $\dot{m}_P$ even on Cartesian grids and, even when exponential terms in the

analytical solution are replaced by the POWER-LAW expressions of Patankar [6].

5. Since the u_{fe} expressions are viewed as models of cell-face velocity, they are also used in the evaluation of convective coefficients (see Eqs. (21)–(24)) without any theoretical justification. In fact, practical experience shows that in order to predict smooth pressure distributions, model expressions are required only in the calculation of $\dot{m}_P$ term; for convective coefficients, simple linearly interpolated expressions for cell-face velocities suffice. This is not surprising because even on staggered grids, the convective coefficients in the cell-face momentum equations are evaluated from linearly interpolated velocities at the cell-faces of the staggered control volumes and which may not satisfy mass conservation for these control volumes.
6. Those who adhere to model expressions for the cell-face velocity for the cure of the zig-zagness problem demonstrate inconsistency of their practice when comparing their numerical predictions with the experimental data. [5] Thus, if for example, experimental data were available at location e (say), the practitioners readily compare their values of $\bar{u}_{\mathrm{e}}$ with the experimental data rather than the model expressions for u_{fe} used in their computer codes.

Thus, it should be clear from the above discussion that the success of the modelled expressions and therefore the very notion of more perfect cell-face velocity modelling itself must be regarded as fortuitous.

3.5. Date's [9] colocated grid form

Since Eq. (32) is applicable to both staggered and colocated grids, the discretised form of the mass conserving pressure correction Eq. (36) is also valid on both types of grids. However, since momentum equations are not solved at the cell-faces, the $\dot{m}_P$ term must be evaluated from interpolated cell-face velocities. Thus, Date's [9] derivation begins with

$$\begin{aligned} AP p'_{\mathrm{m,P}} &= AE p'_{\mathrm{m,E}} + AW p'_{\mathrm{m,W}} + AN p'_{\mathrm{m,N}} + AS p'_{\mathrm{m,S}} \\ &\quad - \bar{\dot{m}}_P + \dot{m}_R \end{aligned} \tag{48}$$

$$\begin{aligned} \bar{\dot{m}}_P &= (\rho_{\mathrm{e}}\bar{u}^l_{\mathrm{e}} - \rho_{\mathrm{w}}\bar{u}^l_{\mathrm{w}})\Delta y + (\rho_{\mathrm{n}}\bar{v}^l_{\mathrm{n}} - \rho_{\mathrm{s}}\bar{v}^l_{\mathrm{s}})\Delta x \\ &\quad + (\rho_P^{l+1} - \rho_P^{\mathrm{o}})\frac{\Delta}{\Delta t} \end{aligned} \tag{49}$$

and $\dot{m}_R$ is already defined in Eq. (39). The task now is to represent velocities and the residuals at the cell-faces in terms of nodal values. Here, the cell-face quantities are represented by *multidimensional* averaging. Thus at the cell-face e, for example,

$$\begin{aligned} \bar{u}^l_{\mathrm{e}} &= \frac{1}{2}\left[\frac{1}{2}(u^l_P + u^l_E) + \frac{\Delta y^+ u^l_{\mathrm{se}} + \Delta y^- u^l_{\mathrm{ne}}}{\Delta y^+ + \Delta y^-}\right] \\ u^l_{\mathrm{se}} &= \frac{1}{4}(u^l_P + u^l_E + u^l_S + u^l_{SE}) \\ u^l_{\mathrm{ne}} &= \frac{1}{4}(u^l_P + u^l_E + u^l_N + u^l_{NE}) \end{aligned} \tag{50}$$

Now since the momentum equations are solved at the nodal positions, there is no guarantee that the residuals at the cell-faces will vanish even at convergence. Thus, $\dot{m}_R$ cannot be equated to zero as was done in the staggered grid procedure. Eqs. (34) and (35), however, show that evaluations of $R_{u_{\mathrm{f}}}$ and $R_{v_{\mathrm{f}}}$ will require coefficients A_i corresponding to the cell-face locations. No doubt these can be calculated but, in multi-dimensional flows, this calculation will turn out to be prohibitively expensive. We therefore resort to averaging and write $R_{u_{\mathrm{fe}}}$, for example, as

$$R_{u_{\mathrm{fe}}} = \left.\overline{\frac{(AP^u + BP)u^l_{\mathrm{f}} - \sum A_i u^l_{\mathrm{f}i}}{\Delta}}\right|_{\mathrm{e}} - \frac{BP}{\Delta}u^{\mathrm{o}}_{\mathrm{fe}} + \left.\overline{\frac{\partial p^l}{\partial x}}\right|_{\mathrm{e}} \tag{51}$$

where overbar again denotes multidimensional averaging. Now, again using Eq. (34), we write

$$\left.\overline{\frac{(AP^u + BP)u^l_{\mathrm{f}} - \sum A_i u^l_{\mathrm{f}i}}{\Delta}}\right|_{\mathrm{e}} - \frac{BP}{\Delta}u^{\mathrm{o}}_{\mathrm{fe}} = \overline{R}_{u_{\mathrm{fe}}} - \left.\overline{\frac{\partial p^l}{\partial x}}\right|_{\mathrm{e}} \tag{52}$$

where $\overline{R}_{u_{\mathrm{fe}}}$ is evaluated from equation such as Eq. (50). $\overline{R}_{u_{\mathrm{fe}}}$ thus comprises only of residuals at the nodes for which momentum equations are solved. Thus, $\overline{R}_{u_{\mathrm{fe}}}$ will vanish at convergence [6] and Eq. (52) may be written as

$$\left.\overline{\frac{(AP^u + BP)u^l_{\mathrm{f}} - \sum A_i u^l_{\mathrm{f}i}}{\Delta}}\right|_{\mathrm{e}} - \frac{BP}{\Delta}u^{\mathrm{o}}_{\mathrm{fe}} = -\left.\overline{\frac{\partial p^l}{\partial x}}\right|_{\mathrm{e}} \tag{53}$$

Now the average pressure gradient is also evaluated by multidimensional averaging. Thus

$$\begin{aligned} \left.\overline{\frac{\partial p^l}{\partial x}}\right|_{\mathrm{e}} &= \frac{1}{2}\left[\frac{1}{2}\left(\left.\frac{\partial p^l}{\partial x}\right|_P + \left.\frac{\partial p^l}{\partial x}\right|_E\right) \right. \\ &\quad \left. + \frac{\Delta y^+ \partial p^l/\partial x|_{\mathrm{se}} + \Delta y^- \partial p^l/\partial x|_{\mathrm{ne}}}{\Delta y^+ + \Delta y^-}\right] \\ &= \frac{1}{4}\left[\frac{p^l_E - p^l_W}{\Delta x^+ + \Delta x^-} + \frac{p^l_{EE} - p^l_P}{\Delta x^{++} + \Delta x^+}\right] \\ &\quad + \frac{1}{4}\frac{\Delta y^-}{\Delta y^+ + \Delta y^-}\left[\frac{p^l_E + p^l_{NE} - p^l_P - p^l_N}{\Delta x^+}\right] \\ &\quad + \frac{1}{4}\frac{\Delta y^+}{\Delta y^+ + \Delta y^-}\left[\frac{p^l_E + p^l_{SE} - p^l_P - p^l_S}{\Delta x^+}\right] \end{aligned} \tag{54}$$

To simplify the above evaluations, we introduce the following definitions:

[5] The author has learnt about this inconsistency from practioners. The statement cannot be substantiated on the basis of published information.

[6] This is similar to the practice adopted on staggered grids.

$$\bar{p}_{x,P} = \frac{\Delta x^- p_E + \Delta x^+ p_W}{\Delta x^- + \Delta x^+} \tag{55}$$

$$\bar{p}_{y,P} = \frac{\Delta y^- p_N + \Delta y^+ p_S}{\Delta y^- + \Delta y^+} \tag{56}$$

$$\bar{p}_P = \frac{1}{2}(\bar{p}_{x,P} + \bar{p}_{y,P}) \tag{57}$$

$$\bar{p}_{x,E} = \frac{\Delta x^+ p_{EE} + \Delta x^{++} p_P}{\Delta x^+ + \Delta x^{++}} \tag{58}$$

$$\bar{p}_{y,E} = \frac{\Delta y^- p_{NE} + \Delta y^+ p_{SE}}{\Delta y^- + \Delta y^+} \tag{59}$$

$$\bar{p}_E = \frac{1}{2}(\bar{p}_{x,E} + \bar{p}_{y,E}) \tag{60}$$

Substituting the above equations in Eq. (54), it can be shown that

$$\left.\overline{\frac{\partial p^l}{\partial x}}\right|_{\mathrm{e}} = \frac{1}{2}\left[\frac{p_E^l - p_P^l}{\Delta x^+} + \frac{\bar{p}_E^l - \bar{p}_P^l}{\Delta x^+}\right] = \frac{1}{2}\frac{\partial}{\partial x}(p^l + \bar{p}^l)|_{\mathrm{e}} \tag{61}$$

Therefore, using the foregoing derivations, it follows that Eq. (51)can be written as:

$$R_{u_{\mathrm{fe}}} = -\frac{1}{2}\frac{\partial}{\partial x}(p^l + \bar{p}^l)|_{\mathrm{e}} + \left.\frac{\partial p^l}{\partial x}\right|_{\mathrm{e}} = \left.\frac{\partial p'_{\mathrm{s}}}{\partial x}\right|_{\mathrm{e}} \tag{62}$$

where

$$p'_{\mathrm{s}} = \frac{1}{2}(p^l - \bar{p}^l) \tag{63}$$

A similar excercise at other cell-faces will show that

$$R_{u_{\mathrm{fw}}} = \left.\frac{\partial p'_{\mathrm{s}}}{\partial x}\right|_{\mathrm{w}} \quad R_{v_{\mathrm{fn}}} = \left.\frac{\partial p'_{\mathrm{s}}}{\partial y}\right|_{\mathrm{n}} \quad R_{v_{\mathrm{fs}}} = \left.\frac{\partial p'_{\mathrm{s}}}{\partial y}\right|_{\mathrm{s}} \tag{64}$$

Substituting the above results in Eq. (39)

$$\dot{m}_R = \left(AE\left.\frac{\partial p'_{\mathrm{s}}}{\partial x}\right|_{\mathrm{e}}\Delta x^+ - AW\left.\frac{\partial p'_{\mathrm{s}}}{\partial x}\right|_{\mathrm{w}}\Delta x^-\right) + \left(AN\left.\frac{\partial p'_{\mathrm{s}}}{\partial y}\right|_{\mathrm{n}}\Delta y^+ - AS\left.\frac{\partial p'_{\mathrm{s}}}{\partial y}\right|_{\mathrm{s}}\Delta y^-\right) \tag{65}$$

Now, using the above equation along with Eq. (49), Eq. (32) can be *effectively* written as

$$\frac{\partial}{\partial x}\left[D_x\frac{\partial p'_{\mathrm{m}}}{\partial x}\right] + \frac{\partial}{\partial y}\left[D_y\frac{\partial p'_{\mathrm{m}}}{\partial y}\right] = \frac{\partial(\rho^{l+1}\bar{u}^l)}{\partial x} + \frac{\partial(\rho^{l+1}\bar{v}^l)}{\partial y} + \frac{\partial\rho^{l+1}}{\partial t} - \frac{\partial}{\partial x}\left[D_x\frac{\partial p'_{\mathrm{s}}}{\partial x}\right] - \frac{\partial}{\partial y}\left[D_y\frac{\partial p'_{\mathrm{s}}}{\partial y}\right] \tag{66}$$

Further simplification

Eq. (66) will now be simplified further by writing

$$\frac{\partial}{\partial x}\left[D_x\frac{\partial p'}{\partial x}\right] + \frac{\partial}{\partial y}\left[D_y\frac{\partial p'}{\partial y}\right] = \frac{\partial(\rho^{l+1}\bar{u}^l)}{\partial x} + \frac{\partial(\rho^{l+1}\bar{v}^l)}{\partial y} + \frac{\partial\rho^{l+1}}{\partial t} \tag{67}$$

where the total pressure correction p' is given by

$$p' = p'_{\mathrm{m}} + p'_{\mathrm{s}} \tag{68}$$

Writing of Eq. (67) is permissible because multipliers of gradients of p'_{m} and p'_{s} in Eq. (66) are identical. Further, when computing on colocated grids, the unknown boundary pressures are linearly extrapolated from their near boundary values. Therefore,

$$\left.\frac{\partial p'_{\mathrm{s}}}{\partial n}\right|_{\mathrm{boundary}} = 0 \tag{69}$$

The above boundary condition is also applicable to p'_{m} (see Eq. (41)). Therefore, Eq. (67) can be solved with

$$\left.\frac{\partial p'}{\partial n}\right|_{\mathrm{boundary}} = 0 \tag{70}$$

Thus Eq. (67) with boundary condition (70) is the pressure correction equation appropriate for colocated grids. The discretised form of this equation is

$$APp'_P = AEp'_E + AWp'_W + ANp'_N + ASp'_S - \dot{\bar{m}}_P \tag{71}$$

Once this equation is solved, p'_{m} distribution can be recovered from the computed p' distribution via Eq. (68) since p'_{s} can be calculated from Eq. (63).

3.6. Compressible flow form

In compressible flows, density is a function of pressure. Therefore

$$\rho^{l+1} = \rho^l + \rho'_{\mathrm{m}} = \rho^l + \frac{p'_{\mathrm{m}}}{RT} = \rho^l + \frac{p' - p'_{\mathrm{s}}}{RT} \tag{72}$$

Making the above substitution and treating $\rho'_{\mathrm{m}}\partial p'_{\mathrm{m}}/\partial x = 0$, etc. it can be shown that the compressible form of Eq. (67) is

$$\frac{\partial}{\partial x}\left[D_x^l\frac{\partial p'}{\partial x} - \frac{p'}{RT}u^*\right] + \frac{\partial}{\partial y}\left[D_y^l\frac{\partial p'}{\partial y} - \frac{p'}{RT}v^*\right] = \frac{\partial}{\partial x}\left[\rho^l\bar{u}^l - \frac{p'_{\mathrm{s}}}{RT}u^*\right] + \frac{\partial}{\partial y}\left[\rho^l\bar{v}^l - \frac{p'_{\mathrm{s}}}{RT}v^*\right] + \frac{\partial\rho^{l+1}}{\partial t} \tag{73}$$

where

$$u_{\mathrm{f}}^* = \bar{u}^l - \frac{D_x^l}{\rho^l}\frac{\partial p'_{\mathrm{s}}}{\partial x} \quad v_{\mathrm{f}}^* = \bar{v}^l - \frac{D_y^l}{\rho^l}\frac{\partial p'_{\mathrm{s}}}{\partial y} \tag{74}$$

Eq. (73) has been successfully used by Date [10] to predict compressible flow with shock using a upwind

differencing scheme. Note that in incompressible flows, the starred velocities are zero. Also, $\rho^{l+1} = \rho^l = \rho$ (say) in incompressible flow. In all further discussion, we shall assume that incompressible flow is under consideration.

4. Comparison of a Date's form with other forms

4.1. Comparison with staggered grid form

It will be appreciated that Eq. (40) for staggered grid and Eq. (67) have the same form. But $p'_{\rm m}$, $u_{\rm f}$ and $v_{\rm f}$ in the former are replaced by p', $\bar{u}$ and $\bar{v}$ in the latter. Further differences can be appreciated from the overall calculation procedure described in Table 1.

The table shows that the SIMPLE procedure on the two types of grids is the same except for step 2 where the mass conserving pressure correction $p'_{\rm m}$ is extracted from *total pressure correction* p' on colocated grids. This extraction, however, is a simple algebraic operation. It will be shown in the next section that $p'_{\rm s}$ provides the necessary smoothing to prevent zig-zag pressure prediction. Hence $p'_{\rm s}$ is called the *smoothing pressure correction*.

Finally, in both procedures, the momentum residuals are evaluated in rms sense from

$$R_\Phi = \left[\sum_{\text{all nodes}} \left\{ (AP + BP)\Phi_P - \left(\sum A_i \Phi_i + S_\Phi \right) \right\}^2 \right]^{0.5} \tag{75}$$

where $\Phi = u$, v (on colocated grids) and $\Phi = u_{\rm f}$, $v_{\rm f}$ (on staggered grids). On staggered grids, the mass residual $R_{\rm m}$ is evaluated from Eq. (38) so that

$$R_{\rm m} = \left[\sum_{\text{all nodes}} (\dot{m}_P)^2 \right]^{0.5} \tag{76}$$

Note that the above evaluation is the same as

$$R_{\rm m} = \left[\sum_{\text{all nodes}} \left(AP p'_{{\rm m},P} - \sum A_i p'_{{\rm m}i} \right)^2 \right]^{0.5} \tag{77}$$

where the coefficients A_i are those given in Eq. (37). On staggered grids, it is of course convenient to evaluate $R_{\rm m}$ from Eq. (76) rather than Eq. (77).

On colocated grids, however, $R_{\rm m}$ cannot be evaluated from Eq. (76) because $\bar{\dot{m}}_P$ is evaluated in terms of interpolated nodal velocities via equation (49) and this $\bar{\dot{m}}_P \neq 0$ even at convergence. It is therefore appropriate to evaluate $R_{\rm m}$ from Eq. (77) on colocated grids because it is this equation that truely represents the mass imbalance. This is an important departure from the staggered grid practice that a casual reader may easily overlook.

4.2. Comparison with the popular forms

The overall calculation procedure employing the more popular forms discussed earlier is the same as that used for colocated grids described above except that the notion of smoothing pressure is not embodied in their conception. Instead, the $\dot{m}_P$ term in their pressure correction equation is evaluated from modelled expressions. There are, however, further differences.

It is possible, for example, to show that the present author's form of the pressure correction equation also implicitly conveys cell-face velocity interpolation. Thus comparison of Eqs. (40) and (66) will show that at cell-face e, for example, the author's form with global under-relaxation α implies that

$$\begin{aligned} u_{\rm fe} &= \bar{u}_{\rm e} - \left(\frac{\rho \alpha \Delta}{AP^u} \right)_{\rm e} \left. \frac{\partial p'_{\rm s}}{\partial x} \right|_{\rm e} \\ &= \bar{u}_{\rm e} - \left(\frac{\rho \alpha \Delta}{AP^u} \right)_{\rm e} \left[\left. \frac{\partial p}{\partial x} \right|_{\rm e} - \frac{1}{2} \left. \frac{\partial (p + \bar{p})}{\partial x} \right|_{\rm e} \right] \end{aligned} \tag{78}$$

where $\bar{u}_{\rm e}$ and $\bar{p}$ are multidimensionally averaged. Note that the above forms were exactly derived. Now, it can be shown that Eq. (44) by Rhie and Chow [13] implies that

Table 1
Simple procedure

	Staggered grid	Colocated grid
1	Guess pressure p^l and solve Eqs. (27) and (28) to obtain $u^l_{\rm f}$ and $v^l_{\rm f}$ distributions	Guess pressure p^l and solve Eqs. (19) and (20) to obtain u^l and v^l distributions
2	Solve Eq. (36) to obtain $p'_{\rm m}$ distribution	Solve Eq. (71) to obtain p' distribution and extract $p'_{\rm m} = p' - p'_{\rm s} = p' - \frac{1}{2}(p^l - \bar{p}^l)$
3	Correct velocities and pressure using $p^{l+1}_P = p^l_P + \beta p'_{{\rm m},{\rm P}}$ $u^{l+1}_{\rm fe} = u^l_{\rm fe} - \frac{D_x}{\rho}(p'_{{\rm m},E} - p'_{{\rm m},P})/\Delta x^+$ $v^{l+1}_{\rm fn} = u^l_{\rm fn} - \frac{D_y}{\rho}(p'_{{\rm m,N}} - p'_{{\rm m,P}})/\Delta y^+$	Correct velocities and pressure using $p^{l+1}_P = p^l_P + \beta p'_{{\rm m},P}$ $u^{l+1}_P = u^l_P - \frac{D_x}{\rho}(p'_{{\rm m},E} - p'_{{\rm m},W})/(2\Delta x)$ $v^{l+1}_P = u^l_P - \frac{D_y}{\rho}(p'_{{\rm m,N}} - p'_{{\rm m,S}})/(2\Delta y)$
4	Check momentum and mass residuals	Check momentum and mass residuals

$$u_{\mathrm{fe}} = \bar{u}_{\mathrm{e}} - \left(\frac{\rho\Delta}{AP^u_{\mathrm{e}}}\right)\left.\frac{\partial p'_{\mathrm{s},x}}{\partial x}\right|_{\mathrm{e}}$$
$$= \bar{u}_{\mathrm{e}} - \left(\frac{\rho\Delta}{AP^u_{\mathrm{e}}}\right)\left[\left.\frac{\partial p}{\partial x}\right|_{\mathrm{e}} - \frac{1}{2}\left.\frac{\partial(p+\bar{p}_x)}{\partial x}\right|_{\mathrm{e}}\right] \quad (79)$$

where $\bar{u}_{\mathrm{e}}$ and $\bar{p}_x$ (see Eq. (55)) are one-dimensionally averaged. Note, however, that the terms in the square brackets are not multiplied by α as in Eq. (78). It is this negligence (probably a result of intuitive postulation of Eq. (44)) that led Majumdar [20] to propose a modification to obtain α—independent solutions by adding extra terms in the Peric's form (Eq. (47)). Eq. (79), however, shows that the same effect can be achieved quite easily in the Rhie and Chow form by multiplying the square bracket by α.

5. The notion of smoothing pressure correction

It is now important to validate the notion of the smoothing pressure correction p'_{s} (see Eq. (63)) introduced by the author. This will be done in more ways than one.

1. From Eqs. (34) and (64), it follows that

$$R_{u_{\mathrm{f}}} = \frac{(AP^u + BP)u^l_{\mathrm{f}} - \sum A_i u^l_{\mathrm{f}i} - BPu^{\mathrm{o}}_{\mathrm{f}}}{\Delta} + \frac{\partial p^l}{\partial x} = \frac{\partial p'_{\mathrm{s}}}{\partial x} \quad (80)$$

and similarly

$$R_{v_{\mathrm{f}}} = \frac{(AP^v + BP)u^l_{\mathrm{f}} - \sum A_i u^l_{\mathrm{f}i} - BPv^{\mathrm{o}}_{\mathrm{f}}}{\Delta} + \frac{\partial p^l}{\partial y} = \frac{\partial p'_{\mathrm{s}}}{\partial y} \quad (81)$$

When written in differential form, the above equations indeed imply that

$$\sigma_x = -p + p'_{\mathrm{s}} + 2\mu\frac{\partial u}{\partial x} \quad (82)$$

$$\sigma_y = -p + p'_{\mathrm{s}} + 2\mu\frac{\partial v}{\partial y} \quad (83)$$

Therefore

$$\frac{1}{2}(\sigma_x + \sigma_y) = -p + p'_{\mathrm{s}} + \mu\left(\frac{\partial u}{\partial x} + \frac{\partial v}{\partial y}\right)$$
$$= -p + p'_{\mathrm{s}} + \mu\nabla\cdot V \quad (84)$$

Comparison of the above equations with Eqs. (6), (7) and (10) shows that p'_{s} in discretised equations plays the same role as that played by q. Further, p'_{s}, like q, is also invariant with the transformation of the system of coordinates. Also, in the hydrostatic case where the true pressure varies linearly with x and y, p'_{s} like q is exactly zero (see Eqs. (55) and (56)). When the true pressure departs from linearity, however, p'_{s} is finite (at least, on coarse grids). Further, our derivation shows that the value of λ_1 introduced in Eq. (12) must be 0.5 and the implied continuum (not the discretised) value of $\nabla\cdot V$ must be zero when density is constant. [7] On fine meshes, $p \to \bar{p}$ in the discrete space and hence $p'_{\mathrm{s}} \to 0$ as required in the continuum.

2. Note that in the Rhie and Chow model, equations analogous to (82) and (83) will read as

$$\sigma_x = -p + p'_{\mathrm{s},x} + 2\mu\frac{\partial u}{\partial x} \quad (85)$$

$$\sigma_y = -p + p'_{\mathrm{s},y} + 2\mu\frac{\partial v}{\partial y} \quad (86)$$

It will be appreciated that Eqs. (85) and (86) are not acceptable because $p'_{\mathrm{s},x}$ and $p'_{\mathrm{s},y}$ will introduce directional dependence in the evaluation of the normal stresses (see comment 2 in Section 2.1). Thus, from a fluid dynamical stand-point, an important requirement of Stokes's laws is violated.

3. Eq. (55) defines $\bar{p}_{x,P}$. It is easy to show that this definition implies that $\bar{p}_{x,P}$ is an independent solution to $\partial^2 p/\partial x^2|_P = 0$ and similarly $\bar{p}_{y,P}$ is an independent solution to $\partial^2 p/\partial y^2|_P = 0$. Thus, $\bar{p}_P$ as defined in equation (57) is average of the above two independent solutions and also equals $-0.5(\sigma_x + \sigma_y)$. Therefore, $p'_{\mathrm{s}} = 0.5(p - \bar{p})$ represents the required smoothing pressure correction when the true pressure variation departs from linearity. Further, $\bar{p}_P$ is also invariant with the transformation of the coordinate system as required. These interpretations are useful because they enable evaluation of $\bar{p}_P$ on structured curvilinear and unstructured meshes without any ambiguity. Also, evaluation of $\bar{p}_P$ requires address to immediate neighbours of P (that is p_E, p_N, etc.). This is a significant advantage that is also retained when computing on unstructured and structured curvilinear meshes [8,12].
4. It is important to relate p'_{s} to the notion of the so called fourth-order dissipation terms invoked in the solution of unsteady Navier–Stokes equations. This is essentially a variant of the MAC method [4] on colocated grids. In these solutions, even steady flows are solved by the false transient method. For a small time-step, $AP \ll BP$ so that the appropriate pressure correction equation on colocated grids will read as

$$\frac{\partial^2 p'_{\mathrm{m}}}{\partial x^2} + \frac{\partial^2 p'_{\mathrm{m}}}{\partial y^2} = \frac{1}{\Delta t}\left[\frac{\partial(\rho\bar{u}^l)}{\partial x} + \frac{\partial(\rho\bar{v}^l)}{\partial y}\right] - \left[\frac{\partial^2 p'_{\mathrm{s}}}{\partial x^2} + \frac{\partial^2 p'_{\mathrm{s}}}{\partial y^2}\right] \quad (87)$$

[7] Note that in the SIMPLE procedure, attempt is made to satisfy mass conservation to machine accuracy as measured through R_{m}. In constant density flows this implies that $\nabla\cdot V = 0$.

The smoothing pressure correction terms in Eq. (87) will now be discretised assuming uniform grid. Then, it can be shown that

$$\left.\frac{\partial^2 p'_s}{\partial x^2}\right|_P = \frac{1}{2}\left(\frac{p_E - 2p_P + p_W}{\Delta x^2} - \frac{\bar{p}_E - 2\bar{p}_P + \bar{p}_W}{\Delta x^2}\right) \quad (88)$$

Now substituting for the average pressures using definitions such as (57) and (60), it can be shown that

$$\left.\frac{\partial^2 p'_s}{\partial x^2}\right|_P = -\frac{1}{8}\left(\Delta x^2 \left.\frac{\partial^4 p}{\partial x^4}\right|_P + \Delta y^2 \left.\frac{\partial^4 p}{\partial x^2 \partial y^2}\right|_P\right) \quad (89)$$

A similar derivation for $\partial^2 p'_s/\partial y^2|_P$ will show that

$$\frac{\partial^2 p'_s}{\partial x^2} + \frac{\partial^2 p'_s}{\partial y^2} = -\frac{1}{8}\left[\Delta x^2 \frac{\partial^4 p}{\partial x^4} + (\Delta x^2 + \Delta y^2)\frac{\partial^4 p}{\partial x^2 \partial y^2} + \Delta y^2 \frac{\partial^4 p}{\partial y^4}\right] \quad (90)$$

Note that the right-hand side of the above equation contains cross-derivative terms not found in [24]. This is because, multidimensional averaging practice has been adopted in the author's work. The terms on the right-hand side of Eq. (90) are called the fourth-order dissipation terms and they tend to zero as the mesh size is refined. The same conclusion was attributed to p'_s.

5. It is also important to show the relevance of the smoothing pressure correction to the Predictor–Corrector methods such as the projection method or the PISO method [18]. These methods employ a Poisson's equation for pressure rather than for pressure-correction. In these methods, Eqs. (19) and (20) are solved at the nodes in the predictor stage employing pressure at the old time step. The velocity field so determined is called the * velocity field. Thus

Predictor stage

$$(AP^u + BP)u_P^* = \sum A_i u_i^*|_P + BPu_P^{\circ} + a_P^u(p_W^{\circ} - p_E^{\circ}) \quad (91)$$

$$(AP^u + BP)v_P^* = \sum A_i v_i^*|_P + BPv_P^{\circ} + a_P^v(p_S^{\circ} - p_N^{\circ}) \quad (92)$$

Corrector stage

In this stage, momentum equations at the cell-faces are *postulated* and a new ** velocity field is imagined. Then

$$(AP^u + BP)_e u_{fe}^{**} = \sum A_i u_{fi}^*|_e + BP_e u_{fe}^{\circ} + a_e^u(p_P^* - p_E^*) \quad (93)$$

$$(AP^u + BP)_w u_{fw}^{**} = \sum A_i u_{fi}^*|_w + BP_w u_{fw}^{\circ} + a_w^u(p_W^* - p_P^*) \quad (94)$$

$$(AP^v + BP)_n v_{fn}^{**} = \sum A_i v_{fi}^*|_n + BP_n v_{fn}^{\circ} + a_n^v(p_P^* - p_N^*) \quad (95)$$

$$(AP^v + BP)_n v_{fs}^{**} = \sum A_i v_{fi}^*|_s + BP_s v_{fs}^{\circ} + a_s^v(p_S^* - p_P^*) \quad (96)$$

In the above equations, p^* field is unknown. The **-velocity field is now subjected to mass-conservation constraint. Thus

$$\rho_e a_e^u u_{fe}^{**} - \rho_w a_w^u u_{fw}^{**} + \rho_n a_n^v v_{fn}^{**} - \rho_s a_s^v v_{fs}^{**} + (\rho_P - \rho_P^{\circ})\frac{\Delta}{\Delta t} = 0 \quad (97)$$

Substitution of Eqs. (93)–(96) in Eq. (97) results in an equation for p^*. This equation reads as

$$APp_P^* = AEp_E^* + AWp_W^* + ANp_N^* + ASp_S^* - \dot{m}_P \quad (98)$$

where the coefficients are the same as those given in Eq. (37) and $\dot{m}_P$ is given by

$$(\rho_P - \rho_P^{\circ})\frac{\Delta}{\Delta t} + \rho_e a_e^u\left(\sum A_i u_{fi,e}^* + BP_e u_{fe}^{\circ}\right) - \rho_w a_w^u\left(\sum A_i u_{fi,w}^* + BP_w u_{fw}^{\circ}\right) + \rho_n a_n^v\left(\sum A_i v_{fi,n}^* + BP_n v_{fn}^{\circ}\right) - \rho_s a_s^v\left(\sum A_i v_{fi,s}^* + BP_s v_{fs}^{\circ}\right) = \dot{m}_P \quad (99)$$

The bracketed terms in the above equation can be evaluated exactly by discretising the momentum equations at the cell-faces. To avoid this expensive evaluation, however, Peric [19] used an approximate representation as follows. Thus for the face e, for example,

$$\sum A_i u_{fi,e}^* + BP_e u_{fe}^{\circ} = \frac{1}{2}\left(\sum A_i u_{i,P}^* + \sum A_i u_{i,E}^*\right) + \frac{1}{2}\left\{(BPu^{\circ})_P + (BPu_E^{\circ})\right\} \quad (100)$$

The above equations require coefficients only at the nodes and, these are known. Thus, $\dot{m}_P$ can be constructed from known quantities. It must be noted, however, that equations such as Eq. (100) have no theoretical justification.

Solution of Eq. (98) gives the new pressure field p^*. The new ** velocity field at the nodes is now evaluated explicitly from

$$(AP^u + BP)u_P^{**} = \sum A_i u_i^*|_P + BPu_P^{\circ} + a_P^u(p_W^* - p_E^*) \quad (101)$$

$$(AP^u + BP)v_P^{**} = \sum A_i v_i^*|_P + BPv_P^{\circ} + a_P^v(p_S^* - p_N^*) \quad (102)$$

This completes one predictor–corrector operation. This operation can be carried out several times at a time step.

The above algorithm can also be executed by introducing the idea of smoothing pressure correction. Thus, following Eqs. (34) and (62), it can be shown that Eq. (100) can be written as

$$\sum A_i u^*_{\mathrm{f}i,\mathrm{e}} + BP_{\mathrm{e}} u^{\mathrm{o}}_{\mathrm{fe}} = (AP^u + BP)_{\mathrm{e}} \bar{u}_{\mathrm{e}} + \Delta_{\mathrm{e}} \left\{ \frac{\partial p^0}{\partial x} - \frac{1}{2} \frac{\partial (p^0 - \bar{p}^{\mathrm{o}})}{\partial x} \right\} \tag{103}$$

where $\bar{u}_{\mathrm{e}}$ is given by Eq. (50) and superscript o applies for the first predictor step. Substitution of the equations of the above type in Eq. (99), it can be shown that an equation for a modified pressure p^*_{mod} can be derived. The equation reads as

$$AP p^*_{\mathrm{mod},P} = AE p^*_{\mathrm{mod},E} + AW p^*_{\mathrm{mod},W} + AN p^*_{\mathrm{mod},N} + AS p^*_{\mathrm{mod},S} - \dot{\bar{m}}_P \tag{104}$$

where $\dot{\bar{m}}_P$ is given by Eq. (42). After solving the above equation, the p^* field can be recovered as

$$p^*_P = p^*_{\mathrm{mod},P} + \frac{1}{2}(p^{\mathrm{o}}_P + \bar{p}^{\mathrm{o}}_P) \tag{105}$$

The cell-averaged $\overline{p^{\mathrm{o}}}_P$ can be calculated as described earlier.

6. All the derivations so far have been carried out for cell-face centered grid dispositions. Many researchers, however, prefer node-centered grid dispositions. It is necessary therefore to demonstrate applicability of the smoothing pressure correction to the latter dispositions.

When node-centered disposition is employed, the cell-faces are *not* midway between the adjacent nodes. However, when the pressure (or pressure correction) gradients at the cell-faces are discretised, one writes

$$\left.\frac{\partial p}{\partial x}\right|_{\mathrm{e}} = \frac{p_E - p_P}{\Delta x^+} \quad \left.\frac{\partial p}{\partial y}\right|_{\mathrm{n}} = \frac{p_N - p_P}{\Delta y^+} \tag{106}$$

The above evaluations are considered valid because of the assumption of linear variation of pressure between adjacent grid nodes. Mathematically speaking, if the above evaluations are considered *second-order* accurate then the evaluations are *as good as* being expressed as if the cell-faces were located midway between the adjacent nodes.

Thus, if the pressure correction Eq. (67) was to be discretised based on second-order accurate evaluations of gradients of p' at the cell-faces, one must *effectively* assume that the cell-faces were infact located midway between the adjacent grid nodes. This important matter is most often overlooked by researchers adhering to node-centered grid dispositions.

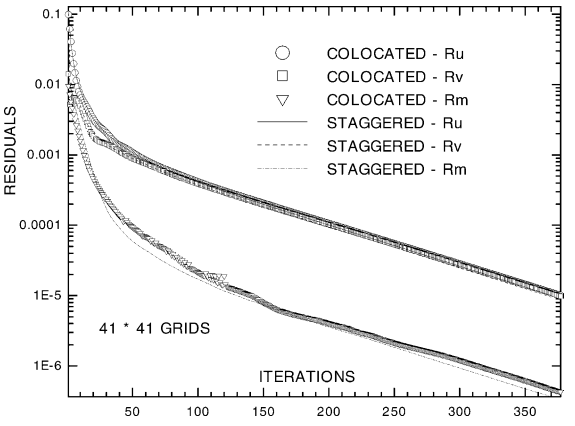

Fig. 3. Convergence histories—square cavity with moving lid-$Re = 100$.

Thus, Eq. (67), along with its discretised form (71), is directly applicable to node-centered grid disposition. The same also applies to evaluations of $\bar{p}$ as indicated in Eqs. (55)–(57).

7. It will be instructive to examine the influence of smoothing pressure correction on the rate of convergence of the overall calculation procedure. To do this, the square cavity problem is solved using staggered and colocated grids. Identical grid size, initial guess and under-relaxation parameters are assumed in the two cases.

Fig. 3 shows variations of R_u, R_v and R_{m} (41×41 grids, $\alpha = 0.5$). It is seen that both colocated and staggered grid computations demonstrate the same convergence rate. The computations were stopped when the momentum residuals were below 10^{-5}. At this level of convergence the mass residuals are seen to be an order of magnitude lower on both grids. Thus, the author's smoothing pressure correction technique does not influence the rate of convergence nor does it influence the level of mass source satisfaction.

6. Conclusions

In this paper, the present author's procedure [9,10] for removing the problem of zig-zag pressure prediction on colocated grids has been comprehensively discussed giving more complete details of algebra. The novel aspect of the procedure is the introduction of *smoothing* pressure correction p'_{s}. The main advantages of the procedure are:

1. Zig-zag prediction is now removed through a simple algebraic operation that retains the smallest computational module throughout the calculation procedure on both structured and unstructured grids.

2. The introduction of smoothing pressure correction offers a more rigorous fluid dynamical view of the problem of zig-zag pressure prediction. The smoothing pressure correction derives from the requirement of Stokes's laws for the normal stresses. In this sense, the paper presents a new expression for the normal stress that is valid for both the continuum as well as the discretised space.
3. The total pressure correction Eq. (67) and the consequent evaluation of p'_s (see Eq. (63)) are valid for both cell-face centered and the node-centered grid dispositions. This must be seen as a natural consequence of the previous conclusion.
4. The notion of smoothing pressure correction is consistent with the so called fourth-order dissipation terms that are commonly introduced in the solution of unsteady Navier–Stokes equations. It is further shown that methods employing Poisson's equation for pressure (rather than pressure-correction) can also be implemented by employing the smoothing pressure-correction.
5. The computed results indicate that the author's pressure smoothing technique has covergence properties that are nearly identical to those possessed by the staggered grid procedure. It is also shown that the mass residual at convergence is also same as that found on staggered grids. On colocated grids, the mass residual must be evaluated from Eq. (77).

References

[1] B.R. Baliga, S.V. Patankar, A control volume finite element method for two-dimensional fluid flow and heat transfer, Numer. Heat Transfer 6 (1983) 245–282.

[2] B.R. Baliga, T.T. Pham, S.V. Patankar, Solution of some two-dimensional incompressible fluid flow and heat transfer problems using a control volume finite element method, Numer. Heat Transfer 6 (1983) 245–282.

[3] S.V. Patankar, D.B. Spalding, A calculation procedure for heat mass and momentum transfer in three dimensional parabolic flows, Int. J. Heat Mass Transfer 15 (1972) 1787–1806.

[4] F.H. Harlow, J.E. Welch, Numerical calculation of time-dependent viscous incompressible flow of fluid with a free surface, Phys. Fluids 8 (1985) 2182.

[5] C. Prakash, S.V. Patankar, A control volume-based finite element method for solving the Navier–Stokes equations using equal-order velocity–pressure interpolation, Numer. Heat Transfer 8 (1985) 259–280.

[6] S.V. Patankar, Numerical Heat Transfer and Fluid Flow, Hemisphere Publishing, New York, 1980.

[7] A.W. Date, Solution of Navier–Stokes equations on non-staggered grid, Int. J. Heat Mass Transfer 36 (1993) 1913–1922.

[8] A.W. Date, Smoothing pressure correction on unstructured mesh, in: Proceedings of 2nd ICHMT Conference on Advances in Computational Heat Transfer, Palm Cove, Australia, May 2001.

[9] A.W. Date, Complete pressure correction algorithm for solution of incompressible Navier–Stokes equations on a non-staggered grid, Numer. Heat Transfer, Part B 29 (1996) 441–458.

[10] A.W. Date, Solution of Navier–Stokes equations on non-staggered grid at all speeds, Numer. Heat Transfer, Part B 33 (1998) 451–467.

[11] A.W. Date, SIMPLE procedure on structured and unstructured meshes with colocated variables, in: Proceedings of the Twelfth International Heat Transfer Conference, Grenoble, France, 2002, pp. 87–92.

[12] S. Ray, A.W. Date, A calculation procedure for solution of incompressible Navier–Stokes equations on curvilinear non-staggered grid, Numer. Heat Transfer, Part B 38 (2000) 93–111.

[13] C.M. Rhie, W.L. Chow, A numerical study of the turbulent flow past an isolated airfoil with trailing edge separation, AIAA J. 21 (1983) 1525–1532.

[14] L. Davidson, A pressure correction method for unstructured meshes with arbitrary control volumes, Int. J. Numer. Methods Fluids 22 (1996) 265–281.

[15] S.R. Mathur, J.Y. Murthy, A pressure-based method for unstructured meshes, Numer. Heat Transfer, Part B 31 (1997) 195–215.

[16] I. Demirdzic, S. Muzaferija, Numerical method for coupled fluid flow, heat transfer and stress analysis using unstructured moving meshes with cells of arbitrary topology, Comput. Methods Appl. Mech. Eng. 125 (1995) 235–255.

[17] T.F. Miller, F.W. Schmidt, Use of a pressure weighted interpolation method for the solution of incompressible Navier–Stokes equations with non-staggered grid system, Numer. Heat Transfer, Part B 14 (1988) 213–233.

[18] R.I. Issa, Solution of implicitly discretised fluid flow equations by operator splitting, J. Comput. Phys. 62 (1986) 40–65.

[19] J.H. Ferziger, M. Peric, Computational Methods for Fluid Dynamics, second revised ed., Springer, London, 1999.

[20] S. Majumdar, Development of a finite volume procedure for prediction of fluid flow with complex irregular boundaries, Report 210/T/29, SFB 210, University of Karlsruhe, Germany, 1986.

[21] D.B. Spalding, A novel finite-difference formulation for differential expressions involving both first and second derivatives, Inter. J. Numer. Methods Eng. 4 (1972) 557–559.

[22] G.D. Thiart, Improved finite-difference scheme for convective–diffusive problems with the SIMPLEN algorithm, Numer. Heat Transfer, Part B 18 (1990) 81–95.

[23] T.M. Shih, A.L. Ren, Primitive variable formulations using non-staggered grids, Numer. Heat Transfer 7 (1984) 413–428.

[24] F. Sotiropolous, S. Abdallah, The discrete continuity equation in primitive variable solutions of incompressible flow, J. Comput. Phys. 95 (1991) 212–227.

[25] H. Schlichting, Boundary-Layer Theory (English translation by J. Kestin), 6th ed., McGraw-Hill, New York, 1968.

[26] Z.U.A. Warsi, Fluid Dynamics—Theoretical and Computational Approaches, CRC Press, London, 1993.